Quantum chaos and analytic structure of the spectrum

W. D. Heiss
Centre for Nonlinear Studies and Department of Physics, University of the Witwatersrand, P.O. Wits 2050, Johannesburg, South Africa

A. A. Kotzé
Centre for Nonlinear Studies and Department of Physics, University of Witwatersrand, P.O. Wits 2050, Johannesburg, South Africa
and Department of Applied Mathematics, Rand Afrikaans University, P.O. Box 524, Johannesburg, South Africa
(Received 15 March 1991)

The intricate connection between the distribution of exceptional points and particular fluctuation properties of level spacings and associated eigenvector statistics is shown. A procedure is given to determine the distribution of the exceptional points of the problem $H_0+\lambda H_1$. Its implementation is demonstrated considering simple matrix models and the quantized chaotic quartic oscillator.

I. INTRODUCTION

The subject "quantum chaos" has attracted a great deal of attention for more than a decade in the literature [1–3]. Yet, a satisfactory definition is still outstanding and may in fact never materialize [4]. It appears that the fascinating properties of systems that are the quantum-mechanical analog of classically chaotic systems still await thorough comprehension, although a lot of experience and understanding has been accumulated. A certain universality in level spacing distributions has been recognized [5] and the applicability of random matrix [6] theory has been demonstrated. The consequences of level statistics upon the statistical behavior of the corresponding eigenstates has also been dealt with more recently [7], as this aspect is particularly relevant for experimental work.

In this paper we attempt to address the question of what the common properties of the *quantum-mechanical operators* are that give rise to spectral properties that are ascribed to quantum chaos. If a matrix representation of a Hamiltonian that originates from a classically chaotic analogy is given, what is the mathematical mechanism that yields the special features of the spectrum within the particular range of the parameter where classical chaos is discerned. While cases with a classical analogy have no intrinsic statistical element, a further puzzling question is as follows: why is it that a statistical approach without physical input reproduces such good agreement of the statistical properties of the spectrum?

We believe that the common root to the answer of these questions lies in what is called the exceptional points [8] of an operator. Most physical problems in quantum mechanics can be formulated by the Hamiltonian $H_0+\lambda H_1$, where the parameter λ can play the role of a perturbation parameter, or it may serve to effect a phase transition, or it may under variation steer the system from an ordered into a chaotic regime. The exceptional points of the full operator are the points λ for which two eigenvalues coalesce. Here we exclude genuine degeneracies of the self-adjoint problem; in other words, the eigenvalues coincide for no real λ. The exceptional points occur in the complex λ plane. Note that the operator is not self-adjoint for complex λ values.

The definition of exceptional points is general and applies in particular to operators in an infinite dimensional space, also when the spectrum of the operator has a continuum part. In the present work we restrict ourselves to finite-dimensional matrices H_0 and H_1, as in this case the role of the exceptional points and the associated Riemann sheet structure is thoroughly understood [9,10]. We do not believe that restriction to matrices has a major impact on our conclusions since virtually all the practical work, even in connection with quantum chaos, is done in a finite-dimensional matrix space.

The physical significance of the exceptional points is due to their relation with avoided level crossing for real λ values. The spectrum $E_k(\lambda)$, $k=1,\ldots,N$, has branch-point singularities at the exceptional points; in fact, two of the N levels are connected via a square-root branch point. If this happens near to the real λ axis, a level repulsion will occur for the two levels for real λ values. Globally, all the exceptional-point singularities determine the shape of the whole spectrum. There is a nice analogy to the more widely known connection between the pole singularities of the scattering function and the shape of the cross section: similar to the way the positions of the poles, including their statistical properties, determine the measurable cross section, the exceptional points determine the shape of the spectrum, and in particular the occurrences of avoided level crossings. The distribution of the exceptional points will therefore determine the fluctuation properties of level spacings.

The positions of the exceptional points are fixed in the complex λ plane and are determined solely by H_0 and H_1. For large matrices it is prohibitive to determine the positions of the exceptional points. However, it is possible to determine the distribution reasonably well from the

knowledge of the two operators. This is one major aspect of this paper. We further demonstrate by simple examples that a high density of exceptional points is a sufficient prerequisite for the occurrence of quantum chaos. There are still a number of open points, some of which are addressed in the final section.

In the following section we recapitulate the basics about exceptional points for matrices to render the paper self-contained. Section III presents two matrix models to exemplify the distribution of exceptional points and level spacing fluctuations. The effect upon the state vectors is also discussed. In Sec. IV the matrix representation of the quartic chaotic oscillator is investigated along the lines developed in the preceding sections. The paper concludes with a critical assessment.

II. EXCEPTIONAL POINTS AND UNPERTURBED LINES

Avoided level crossing is always associated with exceptional points [9,11–13] if it occurs for the levels $E_k(\lambda)$ of the Hamiltonian $H_0+\lambda H_1$. The exceptional points are square-root branch-point singularities in the complex λ plane. We give an elementary example for illustration and briefly list the essential aspects with regard to exceptional points.

Consider a two-dimensional matrix problem where H_0 is diagonal with eigenvalues ϵ_1 and ϵ_2, while H_1 is represented in the form

$$H_1=UDU^{-1} . \tag{2.1}$$

Here, the diagonal matrix D contains the eigenvalues ω_1 and ω_2 of the matrix H_1 and U is the rotation

$$U=\begin{bmatrix}\cos\varphi & -\sin\varphi \\ \sin\varphi & \cos\varphi\end{bmatrix} . \tag{2.2}$$

The eigenvalues of the problem $H_0+\lambda H_1$ are

$$E_{1,2}(\lambda)=\frac{\epsilon_1+\epsilon_2+\lambda(\omega_1+\omega_2)}{2}\pm R , \tag{2.3}$$

where

$$R=\left[\left[\frac{\epsilon_1-\epsilon_2}{2}\right]^2+\left[\frac{\lambda(\omega_1-\omega_2)}{2}\right]^2 +\tfrac{1}{2}\lambda(\epsilon_1-\epsilon_2)(\omega_1-\omega_2)\cos 2\varphi\right]^{1/2} . \tag{2.4}$$

Clearly, when $\varphi=0$ the spectrum is given by the two lines

$$E_k^0(\lambda)=\epsilon_k+\lambda\omega_k, \quad k=1,2 , \tag{2.5}$$

which intersect at the point of degeneracy $\lambda=-(\epsilon_1-\epsilon_2)/(\omega_1-\omega_2)$. When the coupling between the two levels is turned on by switching on φ, the degeneracy is lifted and avoided level crossing occurs. Now the two levels coalesce in the complex λ plane where R vanishes, which happens at the complex-conjugate points

$$\lambda_c=-\frac{\epsilon_1-\epsilon_2}{\omega_1-\omega_2}\exp(\pm 2i\varphi) . \tag{2.6}$$

At these points, the two levels $E_k(\lambda)$ are connected by a square-root branch point; in fact, the two levels are the values of one analytic function on two different Riemann sheets.

These considerations carry over to an N-dimensional problem [9]. The diagonal matrix H_0 contains the elements ϵ_k and D the elements ω_k, $k=1,\ldots,N$; the matrix U is now an N-dimensional rotation, which can be parametrized by $N(N-1)/2$ angles. (In the quoted paper a parametrization was chosen so that U is unity when all angles are zero.) The exceptional points are determined by the simultaneous solution of the equations

$$\begin{aligned}&\det(E-H_0-\lambda H_1)=0 ,\\ &\frac{d}{dE}\det(E-H_0-\lambda H_1)=0 .\end{aligned} \tag{2.7}$$

There are generically $N(N-1)$ solutions that occur in complex-conjugate pairs in the λ plane. At those points the N levels $E_k(\lambda)$ are connected in pairs by square-root branch points when they are analytically continued into the complex λ plane. Since the positions of the singularities determine the shape of the spectrum, and in particular the fluctuation properties, a closer analysis is indicated. As is exemplified in the following section, the crucial condition for the occurrence of level statistics ascribed to quantum chaos is a high density of exceptional points in the complex plane within a small window of real λ values.

To get an idea about the density of exceptional points we introduce the concept of *unperturbed lines*. Clearly, when U is the unit matrix (all angles are zero), the spectrum of $H_0+\lambda H_1=H_0+\lambda D$ is given by the lines of Eq. (2.5) with $k=1,\ldots,N$. The $N(N-1)/2$ intersection points of the N lines depend on the relative order of the numbers ϵ_k and ω_k. If both sequences are in ascending order, all intersections occur at negative λ-values; conversely, if one sequence is ascending and the other descending all intersections occur at positive λ values. In general, the order that is appropriate for the actual problem is expected to lie between the two extremes. To find out the appropriate order we are guided by the asymptotic behavior of the levels $E_k(\lambda)$ of the full problem. For large values of λ the leading terms are given by

$$E_k(\lambda)=\lambda\omega_k+\alpha_k+\cdots , \tag{2.8}$$

where the ellipsis denotes first- and higher-order terms in $1/\lambda$. Neglecting these terms, Eq. (2.8) yields just the unperturbed lines with the appropriate association of slopes ω_k and intercepts α_k. From perturbation arguments we find the latter to be the diagonal elements of the "backwards" rotated H_0, viz.,

$$\alpha_k=(U^{-1}H_0U)_{k,k} . \tag{2.9}$$

We note that a similar procedure for a suitable definition of unperturbed lines was given elsewhere [9], but the procedure proposed here is more efficient to implement and, in fact, the lines as defined here are nearer to the actual spectrum $E_k(\lambda)$.

The significance of Eqs. (2.8) and (2.9) lies in the easy availability of the parameters of the unperturbed lines

from the knowledge of H_0 and H_1 alone. The exceptional points of the full problem are expected to lie near the intersection points of the unperturbed lines (for the two-dimensional problem the real parts of the exceptional points coincide with the points of intersection). Hence, knowledge of H_0 and H_1 alone enables us to predict for which values of λ strong fluctuations of the energy levels are expected to occur and where they definitely do not occur.

III. SIMPLE EXAMPLES

For illustration we present two matrix examples in which typical Gaussian-orthogonal-ensemble (GOE)-type level statistics are generated as well as the associated expected statistical properties of the state vectors. We choose as examples two cases that we consider as the extreme ends of a variety of intermediate possibilities. The one example produces a maximum density of exceptional points within a small window of real λ values, while the other example produces a diluted density over a wide range of real λ values.

A. High density of exceptional points

We start with lines generated by the Hamiltonian matrices (N even)

$$H_0=k\delta_{k,k'} \quad \text{and} \quad H_1=D=\left[\frac{N}{2}-k\right]\delta_{k,k'}, \qquad k=1,\ldots,N, \tag{3.1}$$

which yields all lines intersecting at $\lambda=1$. The fact that we have chosen a harmonic spectrum for both Hamiltonians is immaterial for the following. We now rotate H_1 by an orthogonal matrix U. Similar to the discussion of the two-dimensional case in the preceding section, we now except $N(N-1)/2$ complex-conjugate pairs of exceptional points to emerge from the common intersection point. Clearly the result will depend on the specific choice of the rotation. We return to this aspect in Sec. V. By choosing a random orthogonal matrix where the angles are taken at random from the interval $(-\varphi_0,\varphi_0)$, it turns out that for $N=400$ the nearest-neighbor distribution of the energy levels matches the Wigner surmise for angles as small as $\varphi_0=0.003$. Likewise, the $\Delta_3(L)$ curve, which was investigated for $1\le L\le 12$, moves up from the constant value $\Delta_3=\frac{1}{12}$ to its GOE prediction with increasing φ_0 in a corresponding way. We stress the rather sudden change from a harmonic spectrum to a GOE-type situation. For $\varphi_0=0.003$, these results hold only in the immediate vicinity of $\lambda=1$, while the harmonic nature of the spectrum is left virtually unchanged for λ values further away from unity. The level statistics are based on unfolded spectra.

The behavior of the eigenvectors is in accordance with the observations for the spectrum. The eigenvectors are almost identical to the unperturbed ones for $\lambda\neq 1$. In other words, when ordering the eigenvectors according to an ascending order of the eigenvalues, they form for $\lambda<1$ essentially a unit matrix, while for $\lambda>1$ their order is simply reversed (up to possible minus signs). Note that for $\lambda\to\infty$ the exact form a actually is

$$A(\infty)=U\begin{bmatrix} 0 & & \pm 1 \\ & \ddots & \\ \pm 1 & & 0 \end{bmatrix}, \tag{3.2}$$

where U is the matrix that rotates H_1. Owing to the small value of φ_0, U is very close to a unit matrix. For $\lambda\approx 1$ the eigenvectors change dramatically. The strong mixing of the states brought about by the immediate vicinity of a high density of exceptional points effects a drastic delocalization. As a measure we use the average localization length [7]

$$d=\exp(\langle S\rangle-\langle S_{\mathrm{GOE}}\rangle), \tag{3.3}$$

where $\langle S\rangle$ is the information entropy averaged over all state vectors, viz.,

$$S_k=-\sum_{i=1}^{N} w_{i,k}\ln w_{i,k}, \quad w_{i,k}=|A(\lambda)_{i,k}|^2$$
$$\langle S\rangle=\frac{1}{N}\sum_{k=1}^{N} S_k \tag{3.4}$$

with $A(\lambda)_{i,k}$ containing the eigenvectors as column vectors, and $\langle S_{\mathrm{GOE}}\rangle$ is the corresponding quantity for a pure random (GOE) orthogonal matrix. For large N its leading term is known to be [7] $\sim\ln N$. With our normalization the average length d is unity for a completely delocalized unit vector and zero (up to $1/N$ terms) for a localized one. The length d is plotted as a function of λ in Fig. 1. Obviously, in the vicinity of $\lambda\approx 1$ it comes close to its maximum value unity, while otherwise it is virtually zero corresponding to the localized eigenvectors, which are essentially of the form $(0\ldots1\ldots0)$. The

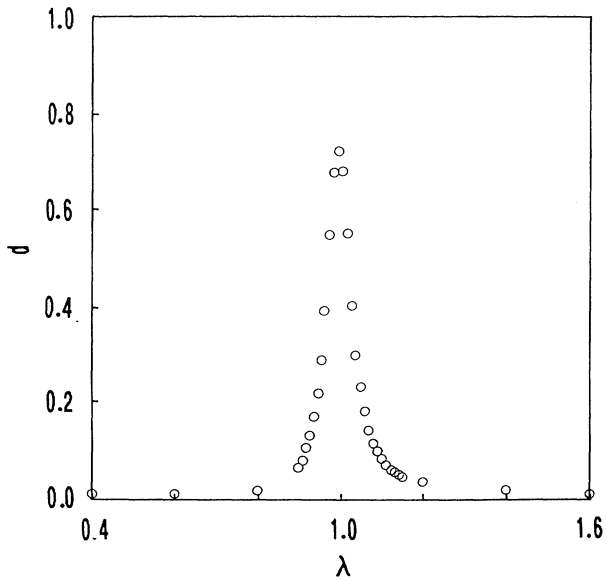

FIG. 1. Average delocalization length of eigenvectors vs λ for $\varphi_0=0.003$ for high density of exceptional points. At $\lambda=1$ most eigenvectors (see Fig. 2) are delocalized, while for λ farther away from unity the eigenvectors are virtually unaffected and of the localized form $(0\ldots1\ldots0)$.

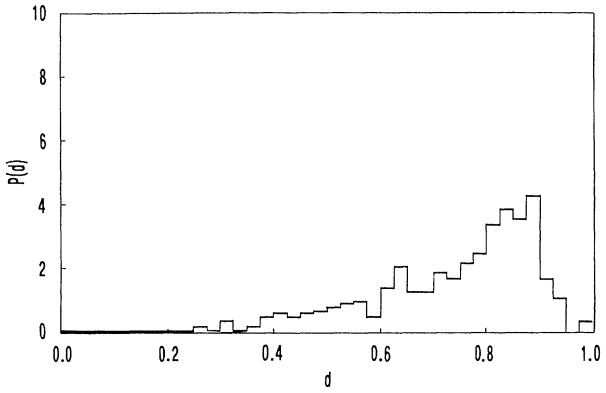

FIG. 2. Distribution of the individual localization lengths for $\lambda=1$ of the average shown in Fig. 1. Note that a few vectors remain localized despite the strong mixing taking place at $\lambda=1$.

width of the bell-shaped curve increases with the maximum angle φ_0. It is of interest to look at the fluctuations of the individual lengths $d_k=\exp S_k$. Their distribution is plotted for $\lambda=1$ in Fig. 2 showing that some eigenvectors are localized while others are completely spread out.

These results are significant for a number of reasons. We note the extremely high sensitivity under variation of the maximal angle φ_0. This was discussed [13] at length in relation to the motion of the exceptional points and its physical effect in quantum chaos. If another set of random numbers is used for the angles, the local values of spectrum and eigenvectors are strongly affected, yet the statistical properties are left unchanged. The same holds under variation of $\varphi_0 \geq 0.003$ at $\lambda=1$.

A reasonable measure for the smallness of the maximum angle is the quantity $N\varphi_0^2$. If this is kept smaller than, say, 0.01, the leading matrix elements of U are 0.99 or larger (always smaller than 1.0). For the value chosen above, it turns out that $\alpha_k \approx \epsilon_k = k$ with the effect that the unperturbed lines as defined in Eq. (2.8) are almost identical to the lines when $\varphi_0=0$. The intersection points of the unperturbed lines occur in an extremely small range of λ values, which corresponds to the high density of exceptional points for the actual finite value of φ_0. However, if φ_0 is increased further and further, the unperturbed lines will eventually form a random set of lines in that the intercepts are randomly distributed. The intersection points will be spread out over a large range of λ values and so will the actual exceptional points. Accordingly, the statistical properties for spectrum and eigenvectors occur now over a large range of λ values. The situation of randomly distributed unperturbed lines appears of interest for its own sake and we turn to it in the following example.

B. Diluted density of exceptional points

We start with the Hamiltonian matrix

$$H_0=k\delta_{k,k'} \quad \text{and} \quad H_1=D=\not{r}\left[\frac{N}{2}-k\right]\delta_{k,k'}, \qquad k=1,\ldots,N, \tag{3.5}$$

where $\not{r}(n)$ is a random permutation of the natural numbers n. The spectrum is given by the lines $E_k^0=k+\lambda\not{r}(N/2-k)$. The corresponding nearest-neighbor distribution is a Poisson distribution for a large range of λ values ($\lambda=0$ excluded). The eigenvectors are all of the form $(0\ldots1\ldots0)$ but their sequence (the column vectors) in the diagonalizing matrix A is randomly distributed. Only for $\lambda>\lambda_{\max}$ are they ordered as in the previous example; by $\lambda_{\max}$ we denote the rightmost intersection point of the levels.

When rotating H_1 to produce level repulsion, it now turns out that a considerably larger value φ_0 is needed to change the Poisson distribution into a Wigner curve. Only for $\varphi_0=0.05$ is the transition about to take place ($N=400$). The $\Delta_3(L)$ curve, when plotted for $1\leq L\leq 15$, has moved down nicely with increasing φ_0 from the straight line $L/15$ to its GOE prediction. In this example the change from the ordered to the chaotic situation is much less dramatic than in the previous example.

The value $\varphi_0=0.05$ implies that U is no longer close to a unit matrix. As a consequence, when comparing with the lines for $\varphi_0=0$ the unperturbed lines are reshuffled since the order of the α_k is different from the order for the $\epsilon_k=k$. However, while this affects substantially the individual positions of the intersection points, it does not change their distribution. As a consequence, the level statistics hold now for a large range of λ values. The consequence for the eigenvector statistics is of a similar nature in that delocalization is found for all $\lambda>0$. From Figs. 3 and 4 we see that for $\varphi_0=0.05$ the delocalization is not as strongly pronounced as in the previous example. Note that the distribution in Fig. 4 shows virtually no contribution for $d>0.6$. The delocalization does become stronger when φ_0 is further increased. It is interesting to note the pattern in Fig. 3: as indicated by the maximum, the mixing for finite λ values brings about a more pronounced delocalization than the one enforced for large λ value. Here we refer to an important difference to the previous example in that delocalization persists even for $\lambda\rightarrow\infty$. The eigenvectors appear in a matrix like the one in Eq. (3.2) but now with a U that effects delocalization. The levels, however, become equidistant for $\lambda\gg\lambda_{\max}$.

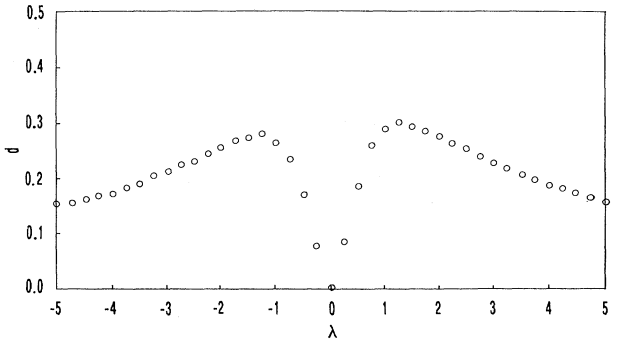

FIG. 3. Average delocalization length for $\varphi_0=0.05$ for the diluted density of exceptional points. Note the maximum at $\lambda\approx\pm1.4$ as discussed in the text.

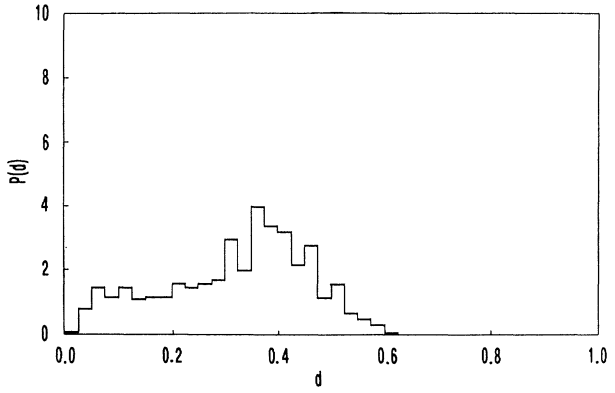

FIG. 4. Individual delocalization length distribution of the diluted density of exceptional points at $\lambda=2.0$. The qualitative pattern persists for a large range of λ values.

IV. THE CHAOTIC QUARTIC OSCILLATOR

To demonstrate our procedure for a physical problem, we have chosen an example that has been addressed by many authors [14–18] from various viewpoints. We choose the Hamiltonians

$$H_0=\tfrac{1}{2}p^2+\tfrac{1}{6}q^4+\tfrac{1}{2}P^2+\tfrac{1}{6}Q^4\ ,$$
$$H_1=-\tfrac{1}{3}q^2Q^2\ , \tag{4.1}$$

so that the full problem $H_0+\lambda H_1$ is equivalent to the Hamiltonians of the quoted papers up to scaling and a rotation of the coordinates. The classical problem is integrable for $\lambda=0$ and becomes fully chaotic at $\lambda=1$. Beyond this point the quantized problem becomes unbounded from below.

The quantum-mechanical treatment is done by matrix diagonalization usually in the harmonic-oscillator basis. To avoid trivial degeneracies in the spectrum, the symmetries are reduced out; we consider the states symmetric under permutation of the lower and upper case coordinates, and of those the positive parity states. In the spirit of our approach we choose H_0 diagonal. This is obviously achieved by diagonalizing it in the standard way. It yields the diagonal elements ϵ_k and the transformation matrix with which to obtain the matrix representation of H_1 in that basis. From the diagonalization of H_1 so obtained we obtain the diagonal matrix D containing the ω_k and the rotation matrix U for which $H_1=UDU^{-1}$. We performed our calculations for $N=1482$. Comparing the spectrum of the full problem with values reported by previous authors confirms that our numerical procedure is safe.

A few comments about the spectrum of H_1 seem adequate. It is known that the operator q^2Q^2 is unbounded and has a continuous spectrum ranging over the whole positive real axis. Any truncated matrix representation is necessarily of a different mathematical nature. In particular, the eigenvalues of the truncated matrix will necessarily depend on the dimension chosen. However, as long as the full problem $H_0+\lambda H_1$ is known to have a discrete spectrum (which is known to be the case for $\lambda\leq 1$), a finite-dimensional matrix representation is expected to yield reliable results at least for the lower part of the spectrum. While this is in fact exploited by everybody who calculates spectra numerically for a physical problem, the importance for our approach lies in the fact that we now consider the matrix problem on its own without reference to its original setting. We follow the analysis according to the lines described in the preceding two sections. In other words, we will now find the occurrence of fluctuations that are ascribed to quantum chaos as a property of the matrix operators H_0 and H_1 alone. For the purpose of this paper the original classical counterpart is not of primary concern, yet it is instructive to compare our findings with the available knowledge of the problem.

Knowledge of the ϵ_k, the ω_k, and of U gives the unperturbed lines using Eqs. (2.8) and (2.9). It turns out that the intersection points within the lower third of the relevant energy range are stable under variation of N. A curve depicting the distribution of the number of intersection points within a small window of real λ values versus λ is given in Fig. 5. We discern a pronounced maximum in the vicinity of $\lambda=1$. Intersection points beyond $\lambda=1$ are inherent to the finite-dimensional matrix problem. The maximum at $\lambda=1$ of the distribution becomes more and more pronounced with increasing N. This pattern was found within the range of N values considered and is also intuitively expected: the largest eigenvalues of H_1 certainly increase steadily with increasing N, hence the steepest (negative) slopes of the unperturbed lines increase with increasing N; further, the ratio of the largest eigenvalues of H_0 to those of H_1 tends towards unity with increasing N, which indicates an accumulation of intersection points at $\lambda=1$ with corresponding energy values near zero. In Fig. 6 we illustrate the unperturbed lines for $N=50$; for much larger values of N many more lines would cross the abscissa in close vicinity of $\lambda=1$. We have thus found a maximum density of exceptional points at the parameter value that is known to be the critical value of the classical and the corresponding infinite-

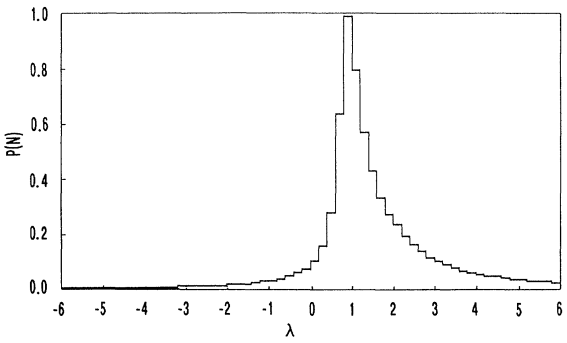

FIG. 5. Number distribution of intersection points of the unperturbed lines for the quartic chaotic oscillator. The normalization is arbitrary; there are further intersections for λ values beyond the range displayed.

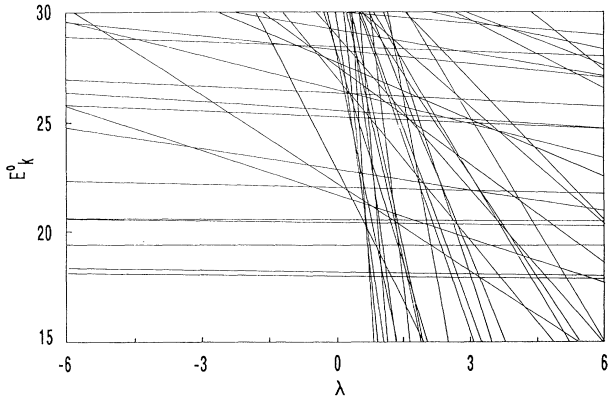

FIG. 6. Pattern of the unperturbed lines of the quartic chaotic oscillator. For the sake of clarity the small value $N=50$ and only a section of the energy range has been chosen. For increasing N more and more intersection points occur in close vicinity of $\lambda=1$.

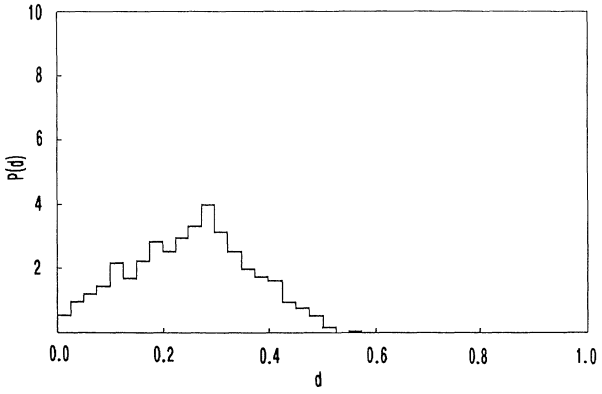

FIG. 8. Individual delocalization length distribution for the quartic chaotic oscillator at $\lambda=0.9$.

dimensional quantum-mechanical problem. Also note that the monotonic increase of the density of intersection points (and thus exceptional points) under variation of λ from 0 to 1 is in line with increasing chaos under such parameter change.

There is an appreciable spread of the density; in other words, the density is not as concentrated as in the example discussed in Sec. III A. This is reflected in the behavior of the eigenvectors of the full problem, which are not as delocalized as in Sec. III A. In Figs. 7 and 8 we present the averaged delocalization length as a function of λ and a distribution function of the individual lengths at $\lambda=0.9$. While the statistical properties of the eigenvectors resemble more those of Sec. III B, the level statistics are known to be in line with GOE results for the λ value considered.

In Fig. 5 a reduced but still substantial density of exceptional points can be noticed for negative values of λ. To the best of our knowledge this region has not been explored, probably since a manifestation of classical chaos is not (easily) visible, although the problem remains as much nonintegrable as for λ positive. From the low density of exceptional points we expect a situation similar to the example in Sec. III B. The analysis of level statistics confirms this nicely in that a distribution is found that is intermediate between a Poisson and a Wigner distribution. The nearest-neighbor spacings can in this case be fitted by Brody [19] distribution. A plot of $\Delta_3(L)$ is illustrated in Fig. 9.

For $\lambda<0$ we found it amusing to increase all the angles of the orthogonal matrix U by a factor 2 [20]. Needless to say, in doing so all contact with the classical problem is lost as the coupling matrix elements are larger on average than the ones prescribed by the original problem.

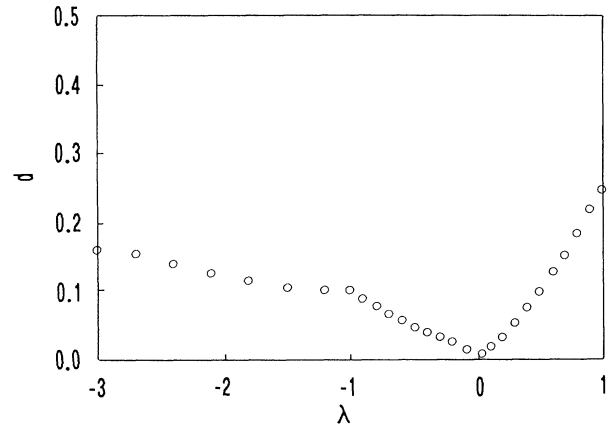

FIG. 7. Average delocalization length for the quartic chaotic oscillator. Note that delocalization is not very strongly pronounced yet substantially stronger for positive λ values than for negative ones.

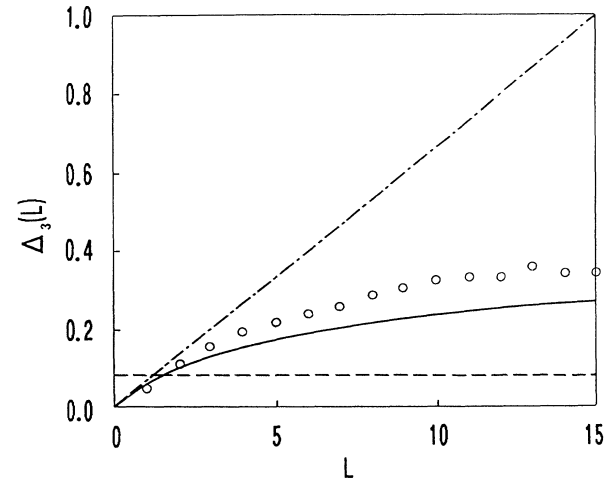

FIG. 9. $\Delta_3(L)$ of the quartic chaotic oscillator at $\lambda=-1.0$. The intermediate character of the curve reflects the corresponding classical situation.

The effect of this operation fulfills all expectations: the emergent level statistic is in agreement with GOE results. The delocalization of the state vectors is enhanced.

V. SUMMARY AND DISCUSSION

The connection between fluctuations in the level spacings and the distribution of the exceptional points of the Hamiltonian $H_0+\lambda H_1$ has been discussed. A procedure to obtain such a distribution by the use of unperturbed lines has been given. The usefulness of the approach has been demonstrated by revisiting the quartic chaotic harmonic oscillator.

The point of view presented in this work is certainly not traditional within the vast literature concerning quantum chaos. While final answers cannot be supplied at this stage, we feel that our contribution does convey a great deal of insight. Below we address a number of points that we believe can be tackled along the lines of this paper.

Even if a high density of exceptional points is found at a certain range of λ values, GOE-type fluctuations must not necessarily occur, although we presume that it is generically the case. In other words, in the example of Sec. III A, some specific nontrivial rotational matrices U could possibly be construed that would produce spectra with little or no fluctuations for the spacings. However, the slightest generic perturbation of that situation would bring back GOE-type fluctuations [13]. It appears that the matrix U in the quartic chaotic oscillator is sufficiently generic to generate the GOE-type spectrum, although there is no random element in it. What must be studied in this context is finding the (probably small) set of constellations of exceptional points, which yields no fluctuations, and determining the corresponding rotation matrices U, which produces such a constellation. From our experience we conjecture that this may be possible only for very specific spectra (like harmonic) of both operators, H_0 and H_1. We stress that it is not possible to prescribe a particular set of exceptional points, since there are strong correlations between them [13].

We have found that quantum chaos is the more likely to occur the higher the density of exceptional points. A more quantitative relation between the dimension N, the density of the exceptional points, and the size of the angles determining the rotation U would be desirable. Note that the angles essentially determine the size of the coupling matrix elements while the density of exceptional points with due regard to N is related to an average level spacing. It has been observed [21] that the quotient of these two physical quantities is crucial for the occurrence of quantum chaos.

The most interesting aspects of substructure in Δ_3, namely its possible relationship to existing closed orbits [22] (if the classical analogy is at hand) and the occurrence of scars [23], must, in principle, be contained in the information residing in the exceptional points. More refined investigations that take into account degeneracies or whole groupings of degeneracies of either H_0 or H_1 or both are expected to shed further light upon these equations. A detailed study of the hydrogen atom in a strong magnetic field, analyzed by our approach, could serve as a guideline. Work along these lines is in progress.

We mention that we argued in a previous paper [13] that transitional regions of finite Fermi systems that undergo a phase transition are generically expected to show patterns ascribed to quantum chaos. The procedure also explains why traditional approximation methods like a mean-field approach are bound to fail in these regions. The reasoning is based on the augmented occurrence of exceptional points in the transitional region.

With the approach adopted in this paper, one might try to give a characterization of quantum chaos: quantum chaos is quantum mechanics under special conditions. If avoided level crossing (or tunneling) occurs on a large scale, then quantum chaos is likely to occur. The high sensitivity [13] under generic perturbation of spectrum and state vectors is explained in terms of the high density of exceptional points. In contrast to the classical case, the transition from order to chaos is smooth, although it can be dramatic.

[1] B. Eckardt, Phys. Rep. **163**, 205 (1988).

[2] O. Bohigas and M. J. Giannoni, in *Mathematical and Computational Methods in Nuclear Physics,* edited by J. S. Dehesa *et al.*, Lecture Notes in Physics Vol. 209 (Springer, Berlin, 1984).

[3] *Chaotic Behavior in Quantum Systems,* edited by G. Casati (Plenum, New York, 1985).

[4] M. V. Berry, Phys. Scr. **40**, 335 (1989).

[5] M. V. Berry and M. Robnick, J. Phys. A **19**, 649 (1986).

[6] T. A. Brody, J. Flores, J. B. French, P. A. Mello, A. Pandey, and S. S. M. Wong, Rev. Mod. Phys. **53**, 385 (1981).

[7] F. M. Izrailev, Phys. Rep. **196**, 299 (1990).

[8] T. Kato, *Perturbation Theory of Linear Operators* (Springer, Berlin, 1966).

[9] W. D. Heiss and A. L. Sannino, J. Phys. A **23**, 1167 (1990).

[10] W. D. Heiss and W.-H. Steeb (unpublished).

[11] P. E. Shanley, Ann. Phys. (N.Y.) **186**, 292 (1989).

[12] C. Bender and T. T. Wu, Phys. Rev. D **7**, 1620 (1973).

[13] W. D. Heiss and A. L. Sannino, Phys. Rev. A **43**, 4159 (1991).

[14] B. Eckardt, G. Hose, and E. Pollak, Phys. Rev. A **39**, 3776 (1989).

[15] A. Carnegie and I. C. Percival, J. Phys. A **17**, 801 (1984).

[16] G. K. Savvidy, Nucl. Phys. B **246**, 302 (1984).

[17] H. D. Meyer, J. Chem. Phys. **84**, 3147 (1986).

[18] W.-H. Steeb, J. A. Louw, W. de Beer, and A. A. Kotzé, Phys. Scr. **37**, 328 (1988).

[19] T. A. Brody, Nuovo Cimento **7**, 482 (1973).

[20] An unambigous definition of the angles for an arbitrary orthogonal matrix and an algorithm to determine them is given in Ref. [9].

[21] T. Guhr and H. A. Weidenmüller, Ann. Phys. (N.Y.) **199**, 412 (1990).

[22] H. Friedrich and D. Wintgen, Phys. Rep. **183**, 38 (1989).

[23] E. J. Heller, in *Quantum Chaos and Statistical Nuclear Physics,* edited by T. H. Seligman and H. Nishioka, Lecture Notes in Physics Vol. 263 (Springer, Berlin, 1986).